9463
NACA TN 3168
TECH LIBRARY KAFB, NM
0065836

NATIONAL ADVISORY COMMITTEE FOR AERONAUTICS

TECHNICAL NOTE 3168

A NEW HODOGRAPH FOR FREE-STREAMLINE THEORY

By Anatol Roshko

California Institute of Technology

Washington
July 1954

AFMDC
TECHNICAL LIBRARY
AFL 2811

TECH LIBRARY KAFB, NM
0065836

1T

NATIONAL ADVISORY COMMITTEE FOR AERONAUTICS

TECHNICAL NOTE 3168

A NEW HODOGRAPH FOR FREE-STREAMLINE THEORY

By Anatol Roshko

SUMMARY

In the method of Helmholtz-Kirchhoff for separated flow past a flat plate (normal to the stream) the separation velocity and the "base pressure" are fixed at the free-stream values. In the present treatment a modification is introduced to allow arbitrary separation velocity and base pressure, so that values more in conformity with experiment may be chosen. The solution depends then on the single (base-pressure) parameter k. When k is suitably chosen, the drag and the details of the potential flow near the plate agree well with experiment. The computations depend on a particular choice of free-streamline hodograph, which has the feature that it gives a definite wake width for every value of k. In this way the wake width is correlated with the drag.

The same ideas are applied to work out the free-streamline flows for a circular cylinder and a wedge of 90° vertex angle.

INTRODUCTION

It is remarkable that the problem of flow past bluff bodies, one of the earliest to receive attention, is not yet understood. The early investigators already had very good insight into the problem; and, although considerable experimental and some theoretical information on the matter has been collected since then, there has been little essential progress toward a theoretical formulation. One of the methods used to attack the problem was that of the free-streamline theory, introduced by Helmholtz and extended by Kirchhoff and many others. Kirchhoff's example of flow past a flat plate, normal to the stream, is well-known. The theory is based on the observation that for the configurations in question the flow separates from the body, leaving behind it a wake and creating a pressure drag quite distinct from that due to shearing forces on the surfaces. The main aim of the theory is to find the "free streamlines" defining the wake, outside which the flow is potential, and to compute the resulting pressure drag.

In the Kirchhoff theory there is a basic assumption which results in a considerable loss of reality. This is the assumption that the

velocity on the free streamline at separation is equal to the free-stream velocity U_∞. The pressure at the separation points, and on the "base" of the body, behind the separation points, is then equal to the free-stream pressure. This is not in agreement with experience, which shows that the base pressure is actually always lower than the free-stream value and that the drag is higher than that calculated by the Kirchhoff theory. However, the Helmholtz-Kirchhoff assumption is attractive, in that the velocity all along the free streamline may be considered constant (U_∞) up to infinity, which leads to a simple formulation in the hodograph plane. The theory has been applied to many shapes other than the normal flat plate; in fact, there is a rather extensive literature on the subject. However, in all cases (with the possible exception of cavity flows) the computed results fail to agree with experience, the discrepancy being mainly due to the basic assumption about the separation velocity.

Clearly, if any progress is to be made with the free-streamline theory, it is necessary that the separation velocity be allowed to assume values different from U_∞. The modification required in the theory may be summed up in a single parameter k, which defines the separation velocity $U_S = kU_\infty$ and gives a base-pressure coefficient $C_{pS} = 1 - k^2$. The base-pressure coefficient is always less than zero, corresponding to $k > 1$. Of course, it is not known what value of k should be assumed, but this is a problem that cannot be determined by the free-streamline theory. It must come from other considerations, principally of the dynamics of the wake.

One might doubt that the free-streamline theory is applicable at all, particularly in view of the last remark. To sum up the evidence for and against it, the following experimental observations may be useful: (1) The discontinuity surfaces, or free streamlines, idealized in the theory, are well approximated by the actual shear layers that exist in a real fluid, for some distance downstream of the separation points (ref. 1, p. 553). (2) On the back of the obstacle, downstream of the separation points, the distribution of pressure is remarkably constant for almost any form of bluff body, even the extreme example of a flat plate inclined at small angle of attack (ref. 2 or ref. 3, p. 679). This means that the velocity at the two separation points is the same, a fact which is rather essential to the theory. (3) The shear layers do not continue far downstream as assumed, but "roll up" to form vortices, alternately on each side. This vortex formation occurs behind all bluff bodies, provided there is no interfering barrier between the separated shear layers, at a frequency which is characteristic for each body shape. Fage and Johansen (ref. 4) noted that the vortex frequency for different bluff bodies could be correlated by expressing it as a dimensionless frequency based not on the body dimension but on the distance d' between the shear layers, measured at the section where they become parallel, before "rolling up." Whether or not the vortices are formed, the idea of free streamlines

extending to infinity is unrealistic, for the shear layers diffuse rapidly. Therefore, it appears rather fruitless to be too concerned with the details of the free streamline at infinity; the main aim should be to obtain a solution which is valid near the body. A more realistic way to formulate the problem is as follows:

The flow past a bluff body is considered in two parts. Near the body it may be described by the free-streamline theory, provided that the parameter k is properly chosen. The description of the wake farther downstream must come from other considerations; if it can also be obtained in terms of the parameter k, then a complete solution may be found by joining the two parts.

Even if it is not possible to complete the solution in this way, on theoretical grounds, the results of the free-streamline theory should be quite useful, particularly for correlating various bluff shapes experimentally. For instance, if from a study of one or two cases it can be determined how k depends on wake breadth, condition of the separated shear layers, and so forth, it may be possible to choose the appropriate value of k for any other bluff body. As another example, the relations between "bluffness," drag coefficient, wake breadth, shedding frequency, wake energy, and so forth, might be easily classified.

The Kirchhoff solution for the normal flat plate is reviewed. Then it is shown how a more realistic solution may be obtained by allowing arbitrary base pressures. The examples of a wedge and circular cylinder are also worked out.

The research was conducted at GALCIT under the sponsorship and with the financial assistance of the National Advisory Committee for Aeronautics.

SYMBOLS

$A_1, A_3, \ldots, A_n$
$a_1, a_3, \ldots, a_n$ } constants

$a = \dfrac{k^2 + 1}{k^2 - 1}$

b streamwise distance to section where streamlines become parallel

C_D drag coefficient

C_p	pressure coefficient
C_{ps}	value of C_p at separation point and on base
$\overline{C_p}$	average of C_p (over a surface)
$\overline{C_{pF}}$	average value of C_p on front of plate or wedge
d	breadth of any cylinder measured normal to stream
d'	distance between parallel free streamlines
g,G,H,I,J	functions defined for convenience of calculation, appendix B

$$h = \frac{k^2 - 1}{2k}$$

$$k = q_s/U_\infty$$

L	length of wedge measured along a side
n	wedge-angle parameter, $2\alpha/\pi$
q	magnitude of velocity (dimensionless)
q_s	value of q at separation point
R	Reynolds number
t	intermediate mapping function
U_∞	magnitude of free-stream velocity (dimensionless)
u,v	components of velocity
w	complex stream function, $\varphi + i\psi$
x	streamwise coordinate in real plane
y	coordinate normal to flow
z	dimensionless complex coordinate, $x + iy$

α	half-angle of wedge
β	angular position on cylinder circumference, measured from stagnation point
β_s	angular distance to separation point on circular cylinder
ζ	inverse of complex velocity, $\frac{1}{\nu} = \frac{1}{q} e^{i\theta}$
θ	direction of flow
φ	velocity potential
ν	complex velocity, $qe^{-i\theta}$
ρ	density
τ	Levi Civita plane
χ	intermediate mapping function
ψ	stream function
Ω	intermediate mapping function, $\log_e \zeta$
Ω_k	intermediate mapping function for $k \neq 1$
Ω'	"shaping" term in Ω

KIRCHHOFF PROBLEM

The problem made famous by Kirchhoff was that of the flow past a flat plate set normal to the stream. It will be useful to review his solution, following essentially the notation of Lamb (ref. 3, p. 99). In sketch 1 the z-plane is the plane of the actual flow. The solution

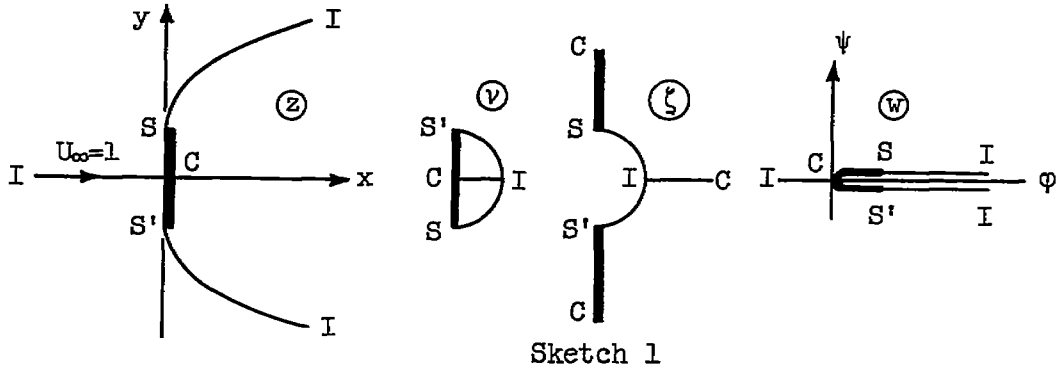

Sketch 1

consists, as usual, of mapping z onto the plane of the complex potential $w = \varphi + i\psi$. This is accomplished through the medium of the complex hodograph or ν-plane, where $\nu = \frac{dw}{dz} = u - iv = qe^{-i\theta}$ is the complex velocity. It is with this plane that the elegance of the Helmholtz-Kirchhoff method is realized. The essential assumption is that everywhere on the free streamlines SI and S'I the velocity is equal to the free-stream value U_∞. Then in the hodograph plane the free streamline is simply the circle $|\nu| = U_\infty$ (= 1 after normalization). Secondly, the trace of the plate SS' in the hodograph plane is known, since the flow direction there is constant. Thus the boundaries of the flow in the hodograph plane are known a priori and are of simple form, so that the mapping to the w-plane is easily accomplished.

In practice it is convenient to use ζ instead of ν, where $\zeta = \frac{1}{\nu} = \frac{1}{q} e^{i\theta} = \frac{dz}{dw}$. Thus ζ gives the true flow direction and the reciprocal of the velocity magnitude at the corresponding point in the physical plane. Once the mappings are known, the solution is given completely by

$$\left.\begin{aligned} z &= \int \zeta \, dw = z(w) \\ q^2 &= \frac{1}{|\zeta|^2} = q^2(w) \end{aligned}\right\} \tag{1}$$

where q^2 determines the pressure, since Bernoulli's equation may be used to evaluate the pressure coefficient

$$C_p = 1 - q^2$$

From relations (1) the pressure everywhere in the flow field may be computed.

In particular, at separation and all along the free streamline $C_p = C_{p_s} = 0$, since $q_s = 1$. The pressure coefficient in the wake and on the back side of the plate is also zero. The drag then is simply due to the excess of pressure on the front; its value in the Kirchhoff example is $C_D = 0.88$.

Now actual experience shows that the drag is considerably larger, being of the order $C_D = 2$; the increase is due mainly to suction on the

back of the plate, $C_{ps} < 0$. Corresponding to this, the velocity on the free streamline at separation is higher than the free-stream value. If $q_s = kU_\infty$, $k > 1$, then $C_{ps} = 1 - k^2$, and the drag contribution from the back side is $k^2 - 1$.

The difference between the computed and the actual drag is a serious discrepancy in the Kirchhoff solution, as well as in the many solutions which have been worked out for various body shapes using the same technique. In other respects, the flow in the immediate vicinity of a flat plate normal to the flow does resemble the conditions anticipated in the theory, as already stated in the "Introduction," so that the free-streamline theory need not be abandoned. It would appear necessary to modify the theory only to the extent of allowing the velocity at separation to assume an appropriate value $q_s = kU_\infty$.

Such an adjustment may be made, in fact, by introducing the hodograph of sketch 2. Here, the velocity at separation is allowed to be $q_s = kU_\infty$

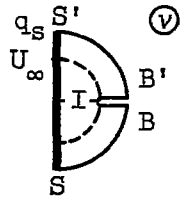

Sketch 2

and to remain at this value along the free streamline (circle in the hodograph plane) until the latter becomes parallel to the free stream (point B in the hodograph plane). At infinity the flow must have returned to the point I, so that the free streamline in the hodograph is simply drawn by joining BI, giving the notch shown in sketch 2. The singularity (doublet) is still at I, as in the Kirchhoff hodograph, which is shown by a dotted line for comparison.

This "notched hodograph" is convenient, for it may be easily mapped onto the w-plane; but it also approximates experiments, since the pressure on the free streamline does tend to remain constant for some distance downstream of the separation point. The solution for flow past a normal flat plate, using this hodograph, is worked out in the next section.

NOTCHED HODOGRAPH

Sketch 3 shows the planes needed to map the flow from the z- to the

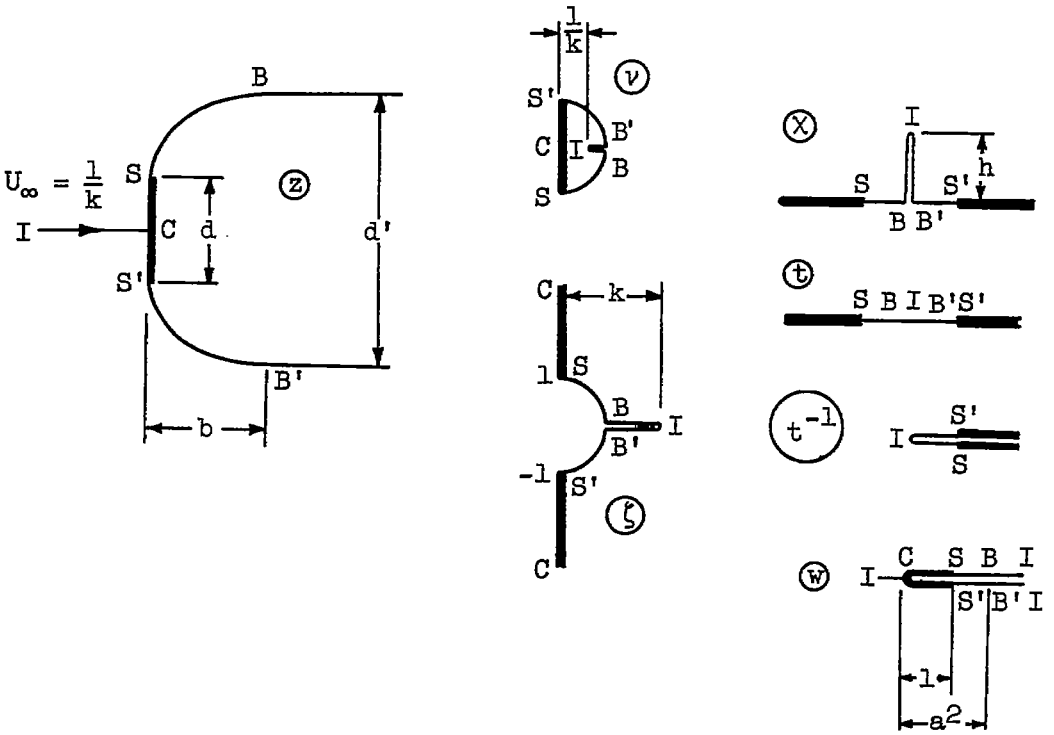

Sketch 3

w-plane, under the assumption that in the hodograph plane it is like sketch 2. To make the radius of the circle in the ν- and ζ-planes equal to unity, the velocity at infinity is set at $U_\infty = 1/k$; that is, $q_s = 1$. The transformations are:

$$\chi = \frac{i}{2}\left(\zeta - \frac{1}{\zeta}\right)$$

which is the Joukowsky transformation,

$$t = \frac{h^2 + \chi^2}{h^2 + 1}$$

where

$$h = \frac{k^2 - 1}{2k}$$

and

$$w = 1/t^2$$

Solving for ζ gives

$$\zeta = -i\left(\chi \pm \sqrt{\chi^2 - 1}\right)$$

$$= -i\sqrt{h^2 + 1}\left(\sqrt{t^2 - \frac{h^2}{h^2 + 1}} \pm \sqrt{t^2 - 1}\right)$$

$$= \pm i \frac{k^2 + 1}{2k}\left(\sqrt{\frac{1}{w} - \frac{1}{a^2}} + \sqrt{\frac{1}{w} - 1}\right) \tag{2}$$

where

$$a = \frac{k^2 + 1}{k^2 - 1}$$

Then,

$$z = \int \zeta \, dw$$

$$= \pm i \frac{k^2 + 1}{2k}\left[\sqrt{w(1 - w)} + \tan^{-1}\sqrt{\frac{w}{1 - w}} + \frac{1}{a}\sqrt{w(a^2 - w)} + a \tan^{-1}\sqrt{\frac{w}{a^2 - w}}\right] \tag{3}$$

the constant of integration having been determined from the condition $z = 0$ at $w = 0$. Relations (2) and (3) give the complete solution.

Of particular interest are points on the plate and along the free streamline, which correspond to real values of $w(=\varphi)$, so that the expressions there are somewhat simplified.

To locate these positions in the physical plane $z = x + iy$, one has from equation (3):

$$\left.\begin{aligned} x &= 0 \qquad\qquad 0 \leqq \varphi \leqq 1 \\ y &= \frac{k^2 + 1}{2k}\left[\sqrt{\varphi(1 - \varphi)} + \tan^{-1}\sqrt{\frac{\varphi}{1 - \varphi}} + \frac{1}{a}\sqrt{\varphi(a^2 - \varphi)} + a \tan^{-1}\sqrt{\frac{\varphi}{a^2 - \varphi}}\right] \end{aligned}\right\} \quad (4)$$

$$\left.\begin{aligned} x &= \frac{k^2 + 1}{2k}\left[\sqrt{\varphi(1 - \varphi)} + \log_e\left(\sqrt{\varphi} + \sqrt{\varphi - 1}\right)\right] \qquad 1 \leqq \varphi \leqq a^2 \\ y &= \frac{k^2 + 1}{2k}\left[\frac{\pi}{2} + \frac{1}{a}\sqrt{\varphi(a^2 - \varphi)} + a \tan^{-1}\sqrt{\frac{\varphi}{a^2 - \varphi}}\right] \end{aligned}\right\} \quad (5)$$

$$\left.\begin{aligned} x &= \frac{k^2 + 1}{2k}\left[\sqrt{\varphi(\varphi - 1)} + \log_e\left(\sqrt{\varphi} + \sqrt{\varphi - 1}\right) + \sqrt{\varphi(\varphi - a^2)} + a \log_e \frac{\sqrt{\varphi} + \sqrt{\varphi - a^2}}{a}\right] \\ y &= \frac{\pi}{2} k \frac{k^2 + 1}{k^2 - 1} \qquad\qquad \varphi \geqq a^2 \end{aligned}\right\} \quad (6)$$

Equations (4), (5), and (6) locate positions on the plate, on the free streamline from S to B, and on the free streamline from B to ∞, respectively. At B the free streamlines become parallel, separated by the distance d', which may be found by putting $\varphi = a^2$ in equations (5) or (6):

$$d' = \pi k \frac{k^2 + 1}{k^2 - 1} \quad (7)$$

Also, the downstream distance to B is

$$b = \left(\frac{k^2 + 1}{k^2 - 1}\right)^2 + \log_e \frac{(k^2 + 1)^2}{k^2 - 1} \tag{7a}$$

The pressure coefficient may be evaluated from

$$C_p = 1 - k^2q^2 = 1 - \frac{k^2}{|\zeta|^2} \tag{8}$$

The values of $|\zeta|^2$ are found from equation (3), which gives, for the positions corresponding to equations (4), (5), and (6) above, the expressions

$$\left.\begin{aligned} |\zeta| &= \frac{k^2 + 1}{2k}\left(\sqrt{\frac{1}{\varphi} - \frac{1}{a^2}} + \sqrt{\frac{1}{\varphi} - 1}\right) && 0 \leqq \varphi \leqq 1 \\ |\zeta| &= 1 && 1 \leqq \varphi \leqq a^2 \\ |\zeta| &= \frac{k^2 + 1}{2k}\left(\sqrt{\frac{1}{a^2} - \varphi} + \sqrt{1 - \frac{1}{\varphi}}\right) && \varphi \geqq a^2 \end{aligned}\right\} \tag{9}$$

To find the drag coefficient, the average pressures on the front and back of the plate are computed:

$$\overline{C_p} = \frac{2}{d}\int_0^{d/2} C_p \, dy = \frac{2}{d}\int_0^1 \left(1 - k^2q^2\right)\frac{1}{q} \, d\varphi \tag{10}$$

where use has been made of the relation

$$dy = \frac{dy}{d\varphi} \, d\varphi = \frac{d\varphi}{q}$$

on the plate. Substituting from equations (9) gives for the average pressure on the front

$$\overline{C_{pF}} = \frac{1}{d}\left[\frac{(k^2 + 1)^2}{k} \tan^{-1} \frac{2k}{k^2 - 1} - 2(k^2 - 1)\right] \tag{11}$$

On the back the pressure is constant, so the average pressure there is simply

$$C_{ps} = 1 - k^2 \tag{12}$$

Finally, the drag coefficient is

$$C_D = \overline{C_{pF}} - C_{ps} \tag{13}$$

The breadth of the plate d is easily found from equations (4) by setting $\varphi = 1$:

$$d = \frac{k^2 + 1}{k}\left(\frac{\pi}{2} + \frac{2k}{k^2 + 1} + \frac{k^2 + 1}{k^2 - 1} \tan^{-1} \frac{k^2 - 1}{2k}\right) \tag{14}$$

The expressions derived above completey describe the flow, for any value of the parameter k. For $k = 1$ they reduce to the Kirchhoff solution. In real flows, however, $k > 1$ and the problem remaining is to choose the correct value. This problem will be returned to later (see the section "Discussion"). First it is necessary to test the validity of the notched hodograph by comparing it with experimental results. For this, there are available some excellent measurements by Fage and Johansen (ref. 2).

COMPARISON WITH EXPERIMENTS AND WITH ANOTHER HODOGRAPH

In one of the cases studied by Fage and Johansen the velocity at the edge of the plate and the pressure on the back correspond to $k = 1.54$. Using this value in equations (8) and (9), the pressure distribution on the front of the plate may be computed and compared with the measured values. Figure 1 shows that the agreement is excellent.

Now it is not at all clear that some other hodograph might not give equally satisfactory agreement, especially since the "end points" of the pressure distribution $\left(C_p = 1 \text{ and } C_{ps} = 1 - k^2\right)$ are fixed once k has been chosen. Any other hodograph curve joining the points S and I (sketch 2) will give the same base pressure coefficient C_{ps} but will otherwise change all the values that have been computed above. To investigate the sensitivity of such a change, SIS' was chosen to be a smooth curve, as shown in sketch 4, defined in such a way that its

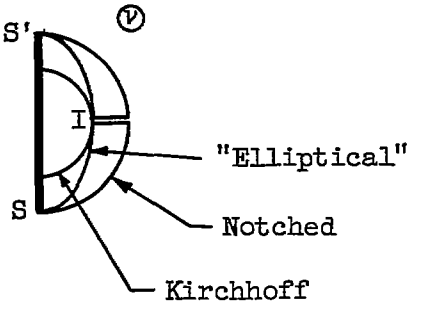

Sketch 4

inverse (in the ζ-plane) is an ellipse. This permits an easy transformation, the details of which are given in appendix A. The pressure distribution on the plate calculated for the "elliptical" hodograph is also shown in figure 1. It does not agree with the measurements so well as does the case of the notched hodograph.

A much more sensitive comparison is given by the pressure distribution along the free streamline, as shown in figure 2(a) for the two cases. The superiority of the notched hodograph is indicated by a comparison with the experimental curve (measured for this purpose), which shows that the pressure tends to remain constant at first, as anticipated. Figure 2(b) shows the streamlines computed for the two hodographs and for the Kirchhoff case. The shaded region is the actual shear layer, measured by Fage and Johansen, which the free streamlines are intended to approximate.

An unusual and very useful feature of the notched hodograph is that the free streamlines become parallel at some section B-B'. In this way a definite value of the wake width d' is defined for every value of k. The definition of a wake width opens some new possibilities which will be taken up later.

Figure 3 shows how the drag coefficient C_D and the wake width d'/d depend on the base-pressure parameter k; the calculated values are given in table I.

After the above method was worked out, the author's attention was drawn to another method, which was given by Riabouchinsky (refs. 5 and 6) and which accomplishes essentially the same thing. Riabouchinsky introduces, further downstream, a second plate which is the mirror image of the first one. The two plates and the two streamlines which join their corresponding edges enclose a region, or cavity, which is assigned an arbitrary pressure. This is then the base pressure, as well as the constant pressure along the free streamline, and may again be specified by the parameter k. For a given k the outer potential flow and the shape of the cavity are given by the theory. The maximum cavity width, which varies with k, may be taken as a measure of the wake width d'. In short, the Riabouchinsky theory, like the notched-hodograph theory, gives a flow which depends on the single parameter k and of which the "front part" may be used to approximate the flow near a bluff plate. For a given base pressure, the drag is very nearly the same as that from the notched-hodograph method, as may be expected. The wake width, however, is somewhat larger, and the free-streamline shape, of course, is somewhat different. The Riabouchinsky theory has been extended to the case of wedges by Plesset and Shaffer (ref. 7), who also found it necessary to use numerical methods to evaluate some of the integrals which occur. It could also be adapted to the case of a circular cylinder, as has been done here for the notched hodograph.

In addition, an early paper by Joukowsky (ref. 8) has recently come to the author's attention. This gives a general method for the case with arbitrary velocity specified along a free streamline. The notched-hodograph results for the bluff plate appear there as a special example and are interpreted as the flow at a channel mouth which is shielded by a flat plate ahead of it.

WEDGES

The results of the preceding section give some confidence that the notched hodograph will also be suitable for other bluff body shapes and that many of the solutions that have been worked out for the Kirchhoff condition $k = 1$ can be generalized in the same way as the case of the normal flat plate. The generalization is straightforward for a wedge of

arbitrary nose angle 2α, shown in sketch 5. For $k = 1$ the problem

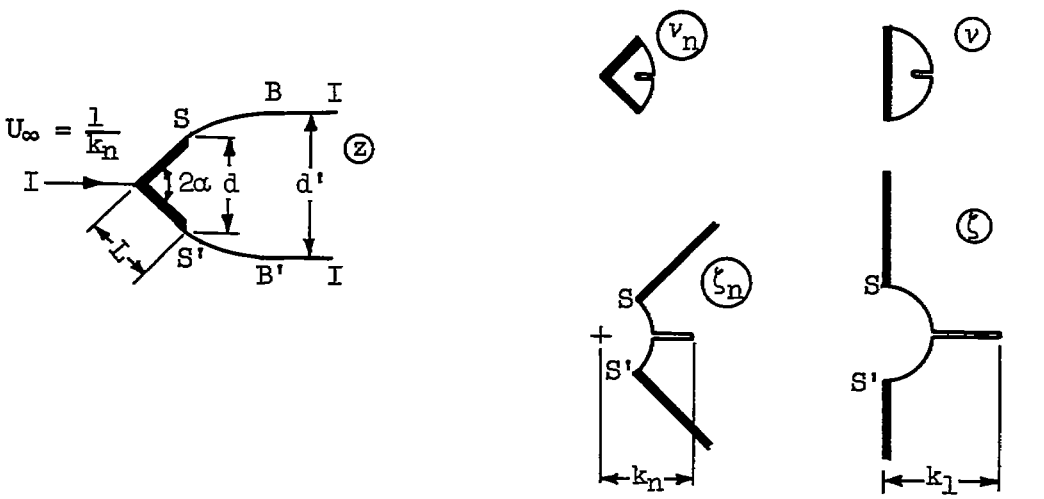

Sketch 5

has been worked out by Bobyleff (see ref. 3, p. 104).

The only additional transformation required is one which will open the segment in the ζ_n-plane onto the half circle in the ζ-plane, from where the mapping to the w-plane is identical with that worked out in the section "Notched Hodograph." The appropriate transformation is

$$\left.\begin{aligned} &\zeta_n = \zeta^n \\ &\text{where} \\ &n = 2\alpha/\pi \qquad 0 \leqq n \leqq 2 \\ &\text{Also, then} \\ &k_1 = k_n^{1/n} \end{aligned}\right\} \tag{15}$$

(The subscripts 1 and n, to distinguish flat plate and wedge, are used to prevent confusion in the transformation; they may be omitted later.) The mapping from w to ζ_n then, referring to equation (2), is

$$\zeta_n = \zeta^n$$

$$= (\pm i)^n \left(\frac{k_1^2 + 1}{2k_1}\right)^n \left(\sqrt{\frac{1}{w} - \frac{1}{a^2}} + \sqrt{\frac{1}{w} - 1}\right)^n \tag{16}$$

The mapping from w to z is

$$z = \int \zeta_n \, dw$$

$$= (\pm i)^n \left(\frac{k_1^2 + 1}{2k_1}\right)^n \int \left(\sqrt{\frac{1}{w} - \frac{1}{a^2}} + \sqrt{\frac{1}{w} - 1}\right)^n dw \tag{17}$$

Since a general solution of the integral in equation (17) could not be found for arbitrary values of n, or even for specific values of n other than 0 or 1, one case ($n = 1/2$, corresponding to $\alpha = 45^\circ$) was worked out numerically. The resulting values for C_D and d'/d, as functions of k, are shown in figure 4 and tabulated in table II. The details for the numerical integration are given in appendix B.

CIRCULAR CYLINDER

In attempting to apply the free-streamline theory to the circular cylinder, two new difficulties are encountered. On the one hand, the trace of the cylinder surface in the hodograph plane is not known a priori. Second, the separation point in the physical plane is not known, as it was in the cases of the plate and wedge. The first difficulty is one only of degree — the mapping may always be accomplished in principle. The problem of the separation point, however, is more difficult; it may be appreciated from the following discussion.

Consider the flow past the curved arc shown in sketch 6. If the

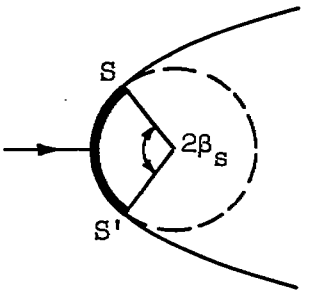

Sketch 6

opening angle $2\beta_s$ is not too large, then separation will occur at S, just as in the case of the flat plate. The curvature of the free streamline at separation will depend on the base pressure coefficient C_{p_s}, that is, on the parameter k. The lower the base pressure, the more sharply will the streamline curve toward the center. As long as the "cylinder" consists only of the curved plate shown by the heavy line, the streamline can adjust itself to any base pressure, always separating at the point S. But if the curved arc is actually part of a complete cylinder, shown dotted, then the radius of curvature of the streamline cannot be smaller than that of the cylinder; otherwise the streamline would intersect the cylinder. It may, of course, be larger. For one particular value of k, that is, of the base pressure, it will be just equal to the radius of the cylinder. If the cylinder is actually the complete one, then β_s is not known a priori; but if it be assumed that the streamline at separation has the same curvature as the cylinder, then there will be a unique value of β_s for every value of k. Thus, with this assumption, a solution may be obtained, depending as in the previous cases only on the parameter k. On the other hand, if the radius of curvature at separation is assumed to be different from (greater than) that of the cylinder, then β_s will be some other function of k. This uncertainty about the conditions at separation makes the free-streamline problem of the cylinder considerably more difficult than the case with fixed separation points.

It seems worth while, as an initial step, to work out the case where the streamline curvature is the same as that of the cylinder. This had already been done for $k = 1$ by Brodetsky (ref. 9) and later by Schmieden (ref. 10). Using a mapping due to Levi Civita, Brodetsky was able to obtain an approximate solution by an iteration procedure which converges quite rapidly. He found the separation to occur at $\beta_s = 55^\circ$, giving a

drag coefficient $C_D = 0.5$. It may be expected that for $k > 1$ the values of β_s and C_D will be higher.

To investigate such arbitrary values of k, Brodetsky's method has been adapted to the notched hodograph. A more complete discussion of the method is given in appendix C. The results are given in figure 5, which shows how the separation point β_s, the drag coefficient C_D, and the distance between streamlines d'/d vary with k. Although the iteration was carried through only one step, the results up to $k = 1.6$ appear to be accurate to a few percent (appendix C). At higher values of k the accuracy (with one iteration) becomes more uncertain, so these have not been plotted.

Figure 6 compares an experimental pressure distribution with one computed on the basis of the above theory for $k = 1.4$, chosen to match the base pressure on the experimental curve. There is considerable improvement over the Kirchhoff case computed by Brodetsky and Schmieden. Only in the vicinity of the separation point is there a serious discrepancy, resulting in quite different values for β_s in the two cases. It is in this region that the uncertainty about the separation condition is most noticeable. Clearly the assumption that the streamline has the same curvature as the cylinder is not satisfactory. With this assumption, there is no adverse pressure gradient (fig. 6), whereas it is well-known that to separate a boundary layer on a continuous surface an adverse gradient is necessary; it exists in the experimental case.

One might, of course, introduce more plausible assumptions about the curvature at separation, but for this it appears necessary to go back to a study of the boundary-layer separation. That the nature of the boundary layer cannot be neglected is clear, since at high Reynolds numbers (above 10^5) the separation point moves to $\beta_s > 90^\circ$. The theory in the above form is suitable only for values less than 90°.

DISCUSSION

In each of the examples treated in the preceding sections, and in every case to which the theory applies, the solution depends on the single parameter k, which cannot be determined without further considerations. In this respect the theory is not closed as is the classical (Kirchhoff) theory, in which it is simply assumed that $k = 1$. That choice of k, however, is arbitrary, and experience shows it to be unrealistic. One might just as well choose a value in much better agreement with experience. For instance, if the value is determined, experimentally, for one bluff body, then it may be used fairly confidently for other shapes at the same Reynolds number; at least the result will be much better than that with

$k = 1$. However, this is a rough observation based on empirical information, not on an essential understanding of the problem. A theoretical or semitheoretical basis (e.g., dimensionless analysis) is needed to choose k, but the free-streamline theory can take one no further in this direction. Some essentially new information must be added; and this, it appears, will not be obtained without a consideration of the wake, the mechanics of which plays a part in setting the base pressure.

Due to the fact that the wakes of different bluff bodies develop in the same way, from the two separated shear layers, they have many features in common. In fact, a wake may be discussed independently of the body if its geometrical and velocity scales are known. This is brought out in Kármán's analysis of the vortex street, in which the two parameters needed to close the problem are a dimension and a velocity (relative to the body). The only function of the body is to determine these two parameters, or scales; it can hardly have any further influence on subsequent developments in the wake (except for Reynolds number effects). That is, the wake is completely determined by a specification of the geometrical and velocity scales early in its development, in the transition from the body regime to the wake regime. The velocity scale may very appropriately be characterized by the velocity along the edges of the free shear layers, while the geometrical scale may be specified by the distance between the free shear layers. These correspond to the parameters k and d'/d. In the free-streamline theory based on the notched hodograph, the relation between k and d'/d is determined, for a given body shape, so that there is only one independent parameter, a result which should prove very useful.

While it may be possible to obtain some results, having only the geometrical and velocity scales of the wake, it will be necessary eventually to consider the Reynolds number effects. These are related principally to the state of the free shear layers, or of the boundary layer before separation. Instead of a Reynolds number based on the body dimension, it will probably be more appropriate to introduce the thickness of the shear layer and its ratio with respect to d'. This problem has received much more attention in the supersonic "base-pressure problem" than in the older problem of incompressible flow past bluff bodies.

Another way in which the results of the notched-hodograph theory may be useful is related to the observations made by Fage and Johansen (ref. 2), already mentioned in the "Introduction." They observed that the frequency of vortex shedding from a bluff body depended not on the dimensions of the body but on the distance between the free shear layers, and they were able to get a good correlation between bodies of different shapes by using this distance in the dimensionless frequency. A single parameter like this might be used, in conjunction with the free-streamline theory and with measurements of the shedding frequency, to determine the drag, for these would give d'/d and thus k and C_D. Here again there

is some dependence on Reynolds number, or rather on the ratio of the shear-layer thickness to d'.

Although there seems to be little possibility at present of obtaining a theoretical description of the mechanics of the wake, especially in the region where it develops from the free shear layers, there is still the possibility of finding a correlation between bodies of different shapes on a semiempirical basis. Since the completion of this work, a study, based on experiment, has been made of the dependence of k on the shear layers and on the distance between them. The free-streamline theory is combined with some experimental results to obtain a correlation between bluff bodies of different shapes, as well as some of the relations between wake and body discussed above. The results of this semiempirical study are presented in reference 11.

California Institute of Technology,
Pasadena, Calif., August 3, 1953.

APPENDIX A

ELLIPTICAL HODOGRAPH

If the free streamline in the ζ-plane is an ellipse (sketch A1),

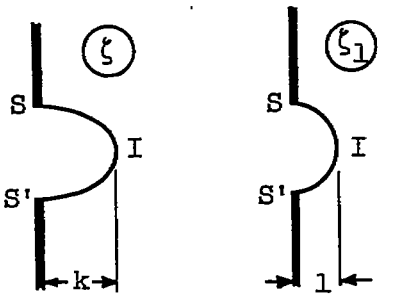

Sketch A1

the mapping to the w-plane is easily found. (Although the corresponding trace of SIS' in the ν-plane (sketch 4) is not an ellipse, it will be conveniently referred to as the elliptical hodograph.)

The ellipse in ζ is first mapped onto the unit circle, in a new plane ζ_1, from where the mapping to the w-plane is the same as that in the Kirchhoff case of figure 1. The first mapping is accomplished by a Joukowsky transformation,

$$\zeta = \frac{1 + k}{2}\zeta_1 + \frac{1 - k}{2\zeta_1}$$

while the second is (cf. eq. (2))

$$\zeta_1 = \pm i\left(\sqrt{\frac{1}{w}} + \sqrt{\frac{1}{w} - 1}\right)$$

These give

$$\zeta = \pm i\left(\sqrt{\frac{1}{w}} + k\sqrt{\frac{1}{w} - 1}\right)$$

$$z = \int \zeta \, dw = \pm i\left[2\sqrt{w} + k\sqrt{w(1 - w)} + k \tan^{-1}\sqrt{\frac{w}{1 - w}}\right]$$

On the plate

$$x = 0$$

$$y = 2\sqrt{\varphi} + k\sqrt{\varphi(1 - \varphi)} + k \tan^{-1}\sqrt{\frac{\varphi}{1 - \varphi}} \qquad 0 \leqq \varphi \leqq 1$$

while on the free streamline

$$x = k\sqrt{\varphi(\varphi - 1)} + \log_e\left(\sqrt{\varphi - 1} + \sqrt{\varphi}\right) \qquad \varphi \geqq 1$$

$$y = k\frac{\pi}{2} + 2\sqrt{\varphi}$$

The breadth of the plate is clearly

$$d = k\pi + 4$$

To evaluate the pressure coefficient given by equation (8),

$$\frac{1}{q} = |\zeta| = \sqrt{\frac{1}{\varphi}} + k\sqrt{\frac{1}{\varphi} - 1} \qquad 0 \leqq \varphi \leqq 1$$

$$= \sqrt{k^2 + \frac{1 - k^2}{\varphi}} \qquad \varphi \geqq 1$$

so that

$$C_p = 1 - \frac{k^2\varphi}{\left(1 + k\sqrt{1 - \varphi}\right)^2}$$

on the plate and

$$C_p = \frac{1 - k^2}{1 - k^2 + k^2\varphi}$$

on the free streamline. The average pressure, computed from equation (10), on the front face is

$$\overline{C_{pF}} = \frac{2}{d}\int_0^1 \left(\frac{1}{q} - k^2 q\right) d\varphi$$

$$= \frac{2}{dk}\pi + 4\sqrt{k^2 - 1}\,\tanh^{-1}\sqrt{\frac{k - 1}{k + 1}}$$

which may then be used to find the drag

$$C_D = \overline{C_{pF}} + k^2 - 1$$

APPENDIX B

MAPPING THE WEDGE

The general mapping for the wedge is given by sketch 5 and relations (16) and (17). Only the wedge surface and the constant-pressure portion of the free streamline will be of particular interest. On these $w = \varphi$ is real and equation (16) reduces to

$$\zeta = e^{i\alpha}\left(\frac{k_1^2 + 1}{2k_1}\right)^n\left(\sqrt{\frac{1}{\varphi} - 1} + \sqrt{\frac{1}{\varphi} - \frac{1}{a^2}}\right)^n \qquad 0 \leqq \varphi \leqq 1 \tag{B1}$$

$$\zeta = e^{i\theta} \qquad 1 \leqq \varphi \leqq a^2 \tag{B2}$$

where

$$\theta = \alpha - n\omega$$

and

$$\omega = \tan^{-1}\sqrt{\frac{\varphi - 1}{1 - \varphi/a^2}}$$

The average pressure normal to one of the front faces, comparing with equation (10), is

$$\overline{C_{pF}} = \frac{1}{L}\int_0^L C_p \, dL = \frac{1}{L}\int_0^1 \left(1 - k^2q^2\right)\frac{1}{q} \, d\varphi \tag{B3}$$

where $1/q = |\zeta|$ in equation (B1). (The subscript has been omitted on k_n but retained on k_1.) The component in the stream direction contributes to the drag the amount $2\overline{C_{pF}} \sin \alpha$. But equation (B3) is averaged on L, whereas it is more convenient to compute the drag with reference to the base dimension $d = 2L \sin \alpha$. On this basis the contribution from the front becomes $\overline{C_{pF}}$, and the drag coefficient is

$$C_D = \overline{C_{pF}} - C_{ps}$$

$$= \overline{C_{pF}} + k^2 - 1$$

The length L of a front face is

$$L = \left(\frac{k_1^2 + 1}{2k_1}\right)^n \int_0^1 \left(\sqrt{\frac{1}{\varphi} - 1} + \sqrt{\frac{1}{\varphi} - \frac{1}{a^2}}\right)^n d\varphi$$

The position of the point B is

$$z_B = Le^{i\alpha} + \int_1^{a^2} e^{i\theta}\, d\varphi$$

In particular, the distance d' between free streamlines, given by the imaginary part of z_B, is

$$d' = 2L \sin \alpha + 2 \int_1^{a^2} \sin \theta \, d\varphi$$

$$= 2L \sin \alpha + 2 \sin \alpha \int_1^{a^2} \cos n\omega \, d\varphi - 2 \cos \alpha \int_1^{a^2} \sin n\omega \, d\varphi$$

and the streamwise distance to B, measured from the base, is

$$b = 2 \cos \alpha \int_1^{a^2} \cos n\omega \, d\varphi + 2 \sin \alpha \int_1^{a^2} \sin n\omega \, d\varphi$$

The above expressions have been reduced to the operations listed in the following summary:

$$G\left(n,k_1\right) = \int_0^1 g \, d\varphi$$

$$H\left(n,k_1\right) = \int_0^1 \frac{1}{g} \, d\varphi$$

$$J\left(n,k_1\right) = \int_1^{a^2} \cos n\omega \, d\varphi$$

$$I\left(n,k_1\right) = \int_1^{a^2} \sin n\omega \, d\varphi$$

where

$$g\left(\varphi;n,k_1\right) = \left(\sqrt{\frac{1}{\varphi} - 1} + \sqrt{\frac{1}{\varphi} - \frac{1}{a^2}}\right)^n$$

$$a^2 = \left(\frac{k_1^2 + 1}{k_1^2 - 1}\right)^2$$

$$n = 2\alpha/\pi$$

$$\omega = \tan^{-1}\sqrt{\frac{\varphi - 1}{1 - \varphi/a^2}}$$

Then

$$L = \left(\frac{k_1^2 + 1}{2k_1}\right)^n G$$

$$\frac{d'}{d} = 1 + \frac{J}{L} - \frac{I}{L} \cot \alpha$$

$$\frac{b}{d} = \cot \alpha \frac{J}{L} + \frac{I}{L}$$

$$\overline{C_{pF}} = \frac{1}{L}\left[\left(\frac{k_1^2 + 1}{2k_1}\right)^n G - k^2\left(\frac{2k_1}{k_1^2 + 1}\right)^n H\right]$$

$$= 1 - k^2\left(\frac{2k_1}{k_1^2 + 1}\right)^{2n} \frac{H}{G}$$

$$C_D = \overline{C_{pF}} + k^2 - 1$$

$$= k_1^{2n}\left[1 - \left(\frac{2k_1}{k_1^2 + 1}\right)^{2n} \frac{H}{G}\right]$$

The solution for given values of k_1 and n corresponds to flow over a wedge of half-angle $\alpha = n\pi/2$ and base-pressure parameter $k = k_1^n$.

APPENDIX C

MAPPING THE CIRCULAR CYLINDER

Brodetsky (ref. 9) shows how the Kirchhoff flow (k = 1) past a curved arc can be computed by means of the mappings shown in sketch C1.

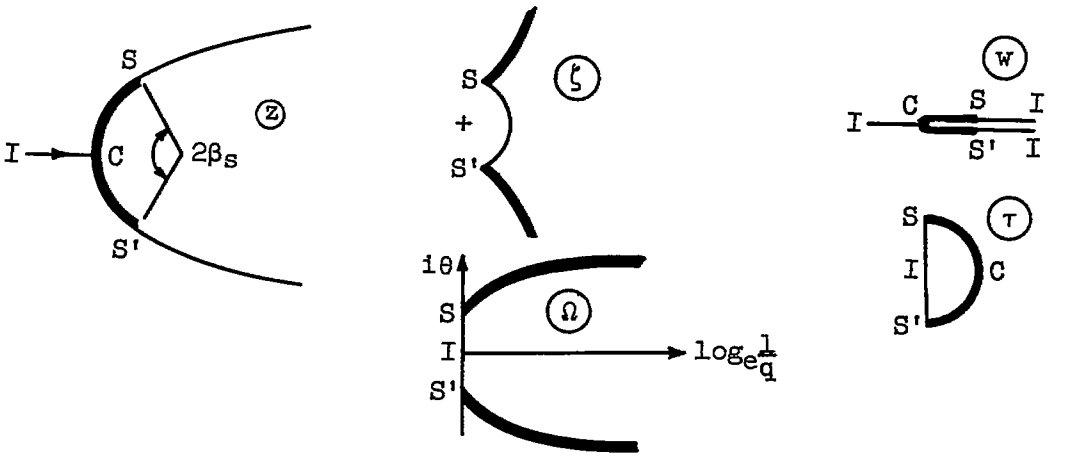

Sketch C1

First, ζ is mapped onto the Ω-plane, often used in free-streamline theory and defined by

$$\Omega = \log_e \zeta = \log_e \frac{1}{q} + i\theta \qquad (C1)$$

The real part of Ω depends only on the magnitude of the velocity, while the imaginary part is the flow direction. The values of θ on the line CS give the flow direction along the surface. For the normal flat plate CS in the Ω-plane would be straight, simply $\theta = i\pi/2$. Now Ω is to be mapped onto the w-plane, and the idea used is that the mapping for the arc may be obtained by adding a "correction" to the mapping for the flat plate, which is known.

To accomplish this, it is helpful to replace w by the Levi Civita[1] plane τ, defined by

$$\sqrt{w} = \frac{\tau^2 - 1}{2i\tau} \tag{C2}$$

In the τ-plane the flow is mapped onto the interior and boundary of the semicircle, which has the doublet at I. For the normal plate the mapping is

$$\Omega = \log_e \frac{1 + \tau}{1 - \tau} \tag{C3}$$

It is assumed that for the curved arc

$$\Omega = \log_e \frac{1 + \tau}{1 - \tau} + \Omega'(\tau) \tag{C4}$$

where Ω' is to be determined. The singularity occurs in the first term so that $\Omega'(\tau)$ may be expressed as a power series,

$$\Omega'(\tau) = A_1\tau + \frac{1}{3} A_3\tau^3 + \cdots \tag{C5}$$

The condition that the streamline curvature at separation should be the same as that of the surface (see the section "Circular Cylinder") is shown by Brodetsky to imply

$$A_1 = -1 + a_1$$

$$A_3 = a_1 + a_3$$

$$A_5 = a_3 + a_5$$

$$\cdots\cdots$$

---

[1]A rather complete discussion of the Levi Civita transformation and of the Ω-plane, as well as applications to the mapping of curved surfaces, is given by Brillouin in reference 12.

that is,

$$\Omega = \log_e \frac{1 + \tau}{1 - \tau} - \left(1 - a_1\right)\tau + \left(a_1 + a_3\right)\tau^3 + \ldots \qquad (C6)$$

To evaluate the a_n's, the radius of curvature of the surface is expressed in terms of them. For a circular arc they are then determined to make the radius of curvature constant on the arc. The solution proceeds by iteration, starting with $a_1 \neq 0$, $a_3 = a_5 = \ldots = 0$. Brodetsky showed that $a_1 = 0.0574$ gives an arc whose radius is constant within $3\frac{1}{2}$ percent, while $a_1 = 0.0585$, $a_3 = -0.0083$ reduces the maximum discrepancy to 0.06 percent. The corresponding values of the separation angle β_s are 55.1° and 55.0°, while the drag coefficients are 0.49 and 0.500, respectively. This indicates that the convergence is quite rapid, a_1 already giving a fairly accurate result. Therefore, in adapting the method to flows where $k > 1$, it was considered sufficient to use only this one term of the iteration.

For $k > 1$, the Ω_k-plane appears as shown in sketch C2, "notched"

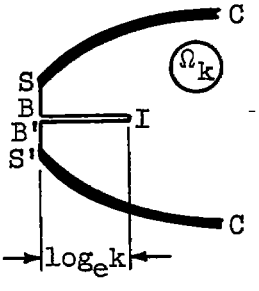

Sketch C2

like the corresponding ζ-plane; that is, along SB the velocity is constant ($q = 1$), while along BI and B'I the streamlines are parallel. Now Ω_k can be mapped onto the Ω-plane (sketch C1) by the transformation

$$\sinh^2 \Omega_k = \left(\frac{k^2 + 1}{2k}\right)^2 \left[\sinh^2 \Omega + \left(\frac{k^2 - 1}{k^2 + 1}\right)^2\right] \qquad (C7)$$

The physical plane corresponding to Ω_k will be called z_k, while that corresponding to Ω is z.

Now the procedure is simply as follows: A value is chosen for a_1. This determines a certain cylinder shape in the z-plane which corresponds to another shape in the z_k-plane. Then k is computed to give a constant radius of the cylinder in the z_k-plane, or as nearly as is possible with only the single term a_1. Thus for each value of a_1 there is a value of k which gives a circular arc in the z_k-plane. The values calculated are given in table III. Each arc has a definite opening angle $2\beta_s$ which determines the corresponding separation angle (sketch C1). The results, referred to already in the section "Circular Cylinder," are plotted in figure 5. Of course, using only a_1 in series (C6), it is not possible to make the arc perfectly circular. All that can be done is to check the accuracy obtained at each value of k. It was found that at $k = 1.6$ the radius is constant within 2 percent and comparable to this at lower values. At higher values of k the accuracy becomes lower; therefore the curves of figure 5 have not been extended beyond $k = 1.6$.

Details of the rather cumbersome calculations for the various quantities are not shown here. They are analogous to those in Brodetsky's paper, with only the additional introduction of transformation (C7) to give the correspondence between the Ω- and Ω_k-planes.

It might be well to point out why it was necessary to introduce this transformation from Ω_k to Ω instead of working directly between Ω_k and τ. With the latter procedure the notch would have been distorted, since the approximate solution attempts only to obtain a fit on the surface SC. In the procedure used, on the other hand, the adjustments are made in the Ω-plane in such a way that the imaginary values on SC are constant in the Ω_k-plane. There is no need then to worry about BIB', for equation (C7) maps it exactly onto the notch in the Ω_k-plane.

REFERENCES

1. Fluid Motion Panel of the Aeronautical Research Committee and Others, (S. Goldstein, ed.): Modern Developments in Fluid Dynamics. Vol. II. The Clarendon Press (Oxford), 1938.

2. Fage, A., and Johansen, F. C.: On the Flow of Air Behind an Inclined Flat Plate of Infinite Span. R. & M. No. 1104, British A. R. C., 1927; also Proc. Roy. Soc. (London), ser. A, vol. 116, no. 773, Sept. 1, 1927, pp. 170-197.

3. Lamb, Horace: Hydrodynamics. Sixth ed., The Univ. Press (Cambridge), 1932.

4. Fage. A., and Johansen, F. C.: The Structure of Vortex Sheets. R. & M. No. 1143, British A. R. C., 1927; also Phil. Mag., ser. 7, vol. 5, no. 28, Feb. 1928, pp. 417-441.

5. Riabouchinsky, D.: On Steady Fluid Motion With Free Surfaces. Proc. London Math. Soc., vol. 19, 1921, pp. 206-215.

6. Riabouchinsky, D.: On Some Cases of Two-Dimensional Fluid Motion. Proc. London Math. Soc., ser. 2, vol. 25, pt. 3, 1926, pp. 185-194.

7. Plesset, M. S., and Shaffer, P. A., Jr.: Cavity Drag in Two and Three Dimensions. Jour. Appl. Phys., vol. 19, no. 10, Oct. 1948, pp. 934-939.

8. Joukowsky, N. E.: I - A Modification of Kirchoff's Method of Determining a Two Dimensional Motion of a Fluid Given a Constant Velocity Along an Unknown Stream Line. II - Determination of the Motion of a Fluid for Any Condition Given on a Stream Line. Works of N. E. Joukowsky, Vol. II, Issue 3, Trans. CAHI, No. 41, 1930. (Originally published in 1890.)

9. Brodetsky, S.: Discontinuous Fluid Motion Past Circular and Elliptic Cylinders. Proc. Roy. Soc. (London), ser. A, vol. 102, no. 718, Feb. 1, 1923, pp. 542-553.

10. Schmieden, C.: Die Unstetige Strömung um einen Kreiszylinder. Ing.-Archiv, Bd. I, Heft 1, Dec. 1929, pp. 104-109.

11. Roshko, Anatol: On the Drag and Shedding Frequency of Two-Dimensional Bluff Bodies. NACA TN 3169, 1954.

12. Brillouin, M.: Sur les surfaces de glissement de Helmholtz. Ann. chimie et phys., ser. 8, vol. 23, 1911, pp. 145-230.

TABLE I

FLAT PLATE

k	$\overline{C_{pF}}$	C_D	d'/d	b/d
1.00	0.880	0.880	∞	∞
1.05	.868	.970	9.460	59.400
1.10	.855	1.065	5.073	15.900
1.15	.843	1.166	3.615	7.600
1.20	.831	1.271	2.888	4.610
1.30	.806	1.496	2.168	2.390
1.40	.782	1.742	1.814	1.570
1.50	.758	2.008	1.606	1.170
1.60	.735	2.295	1.471	.936
1.80	.690	2.930	1.308	.692
2.00	.650	3.650	1.217	.569

TABLE II

90° WEDGE

k	G	H	J	I	$\overline{C_{pF}}$	C_D	d'/d	b/d
1.000	-----	-----	------	------	0.637	0.637	∞	∞
1.106	1.742	0.633	19.870	14.510	.562	.786	4.040	19.540
1.178	1.733	.639	7.370	5.090	.515	.905	2.280	7.800
1.236	1.723	.643	4.390	2.790	.475	1.003	1.889	3.980
1.360	1.710	.649	2.010	1.111	.411	1.261	1.438	1.528
1.452	1.696	.660	1.311	.683	.361	1.471	1.328	1.036

TABLE III

CIRCULAR CYLINDER

a_1	k
0.0574	1.000
.0500	1.175
.0400	1.263
.0200	1.387
0.	1.470
-.0400	1.600

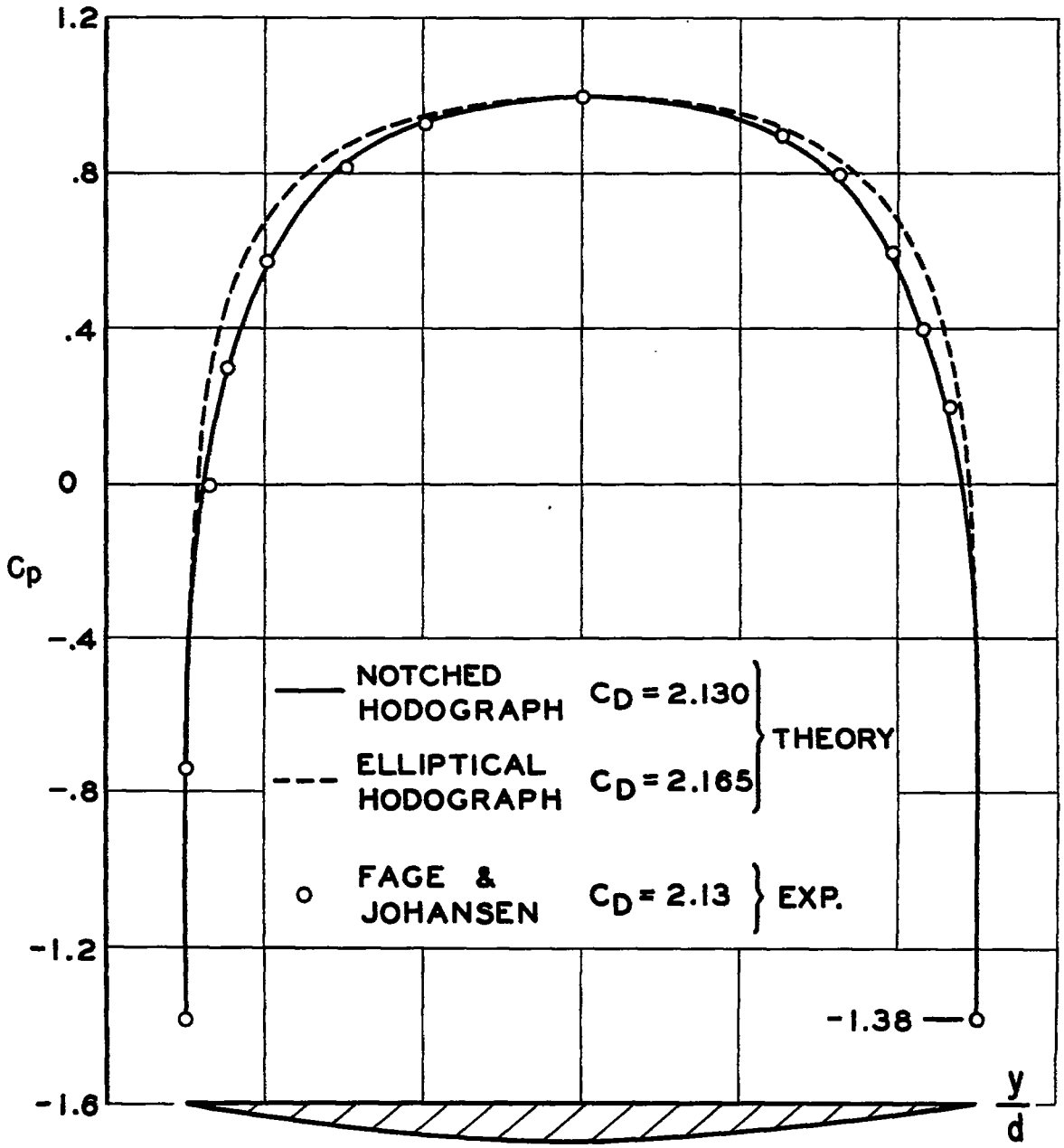

Figure 1.- Pressure on flat plate.

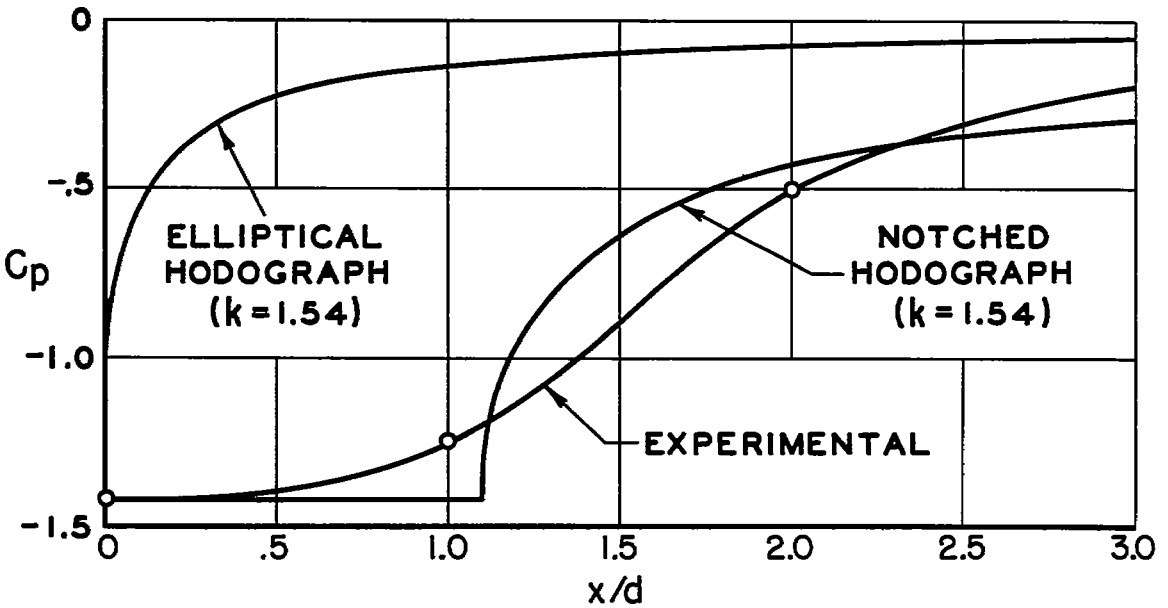

(a) Pressure on free streamline.

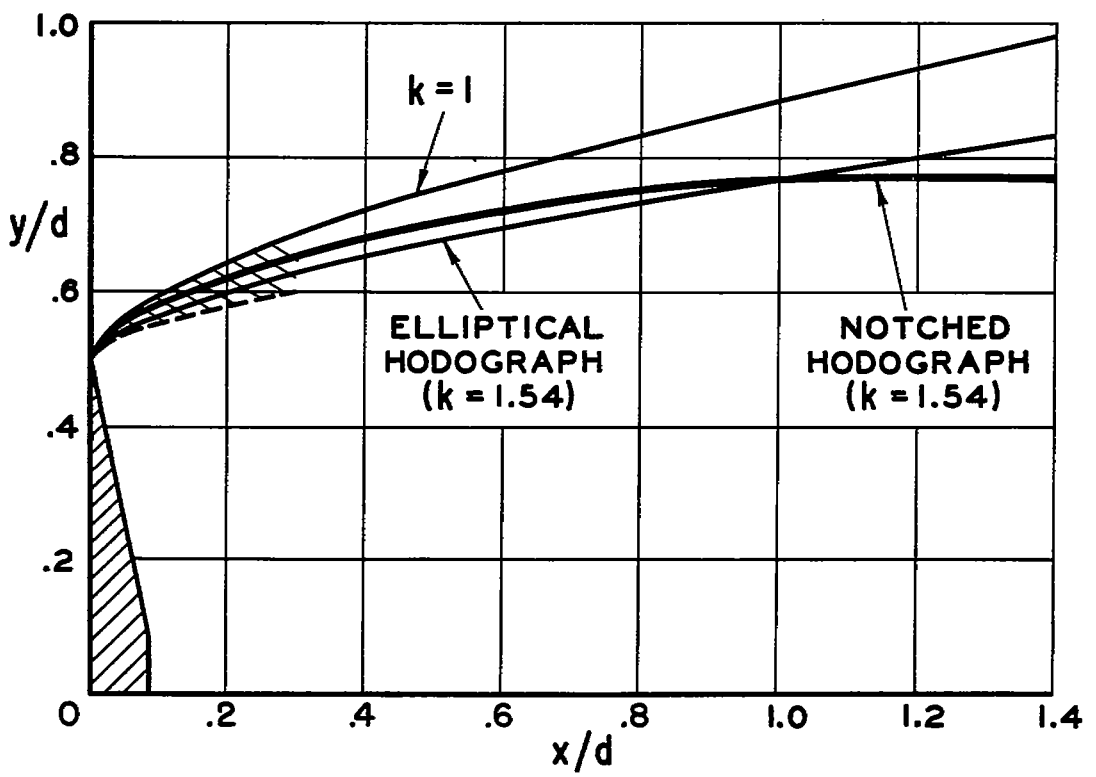

(b) Free streamlines.

Figure 2.- Comparison of elliptical and notched hodographs.

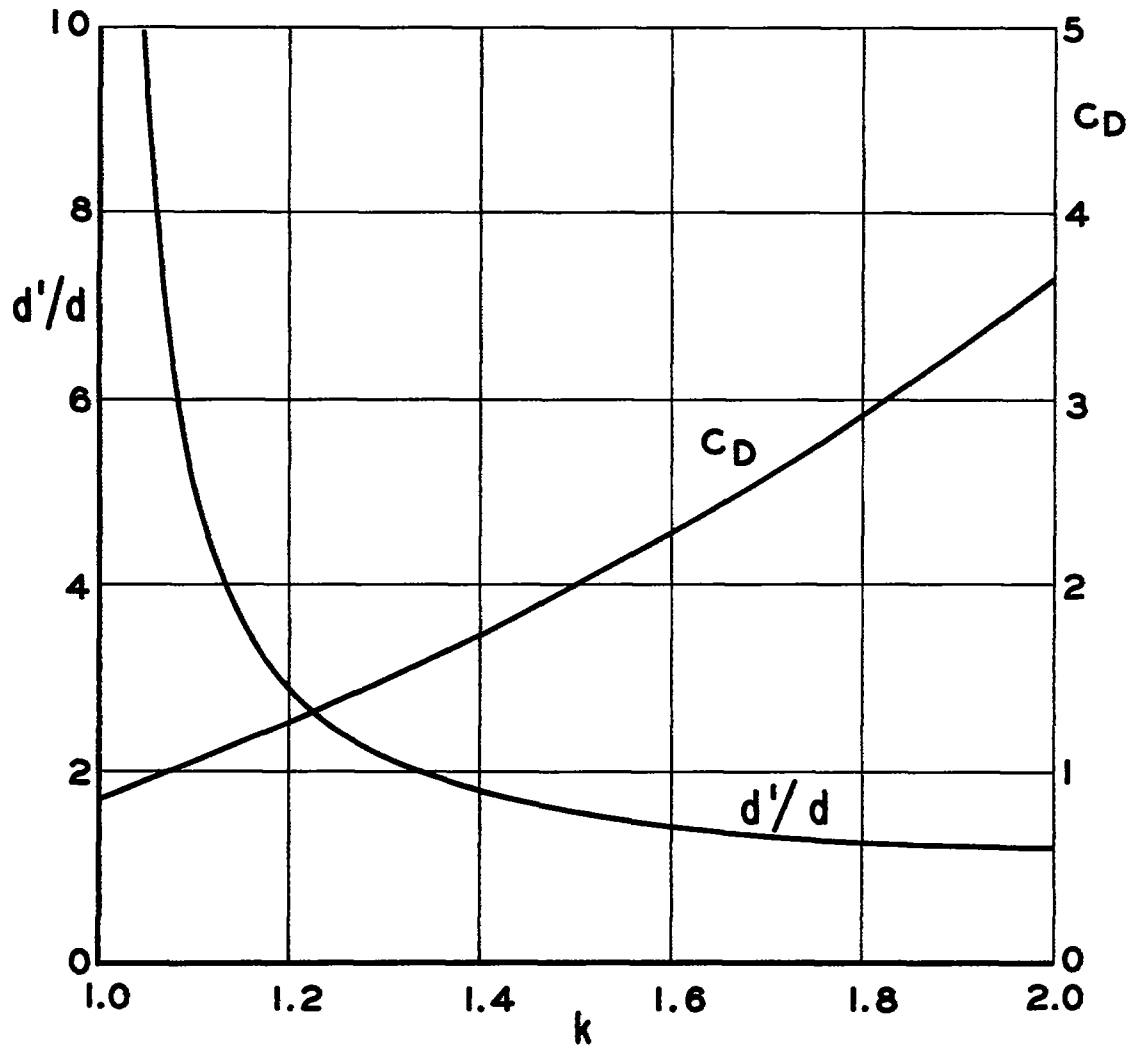

Figure 3.- Normal flat plate.

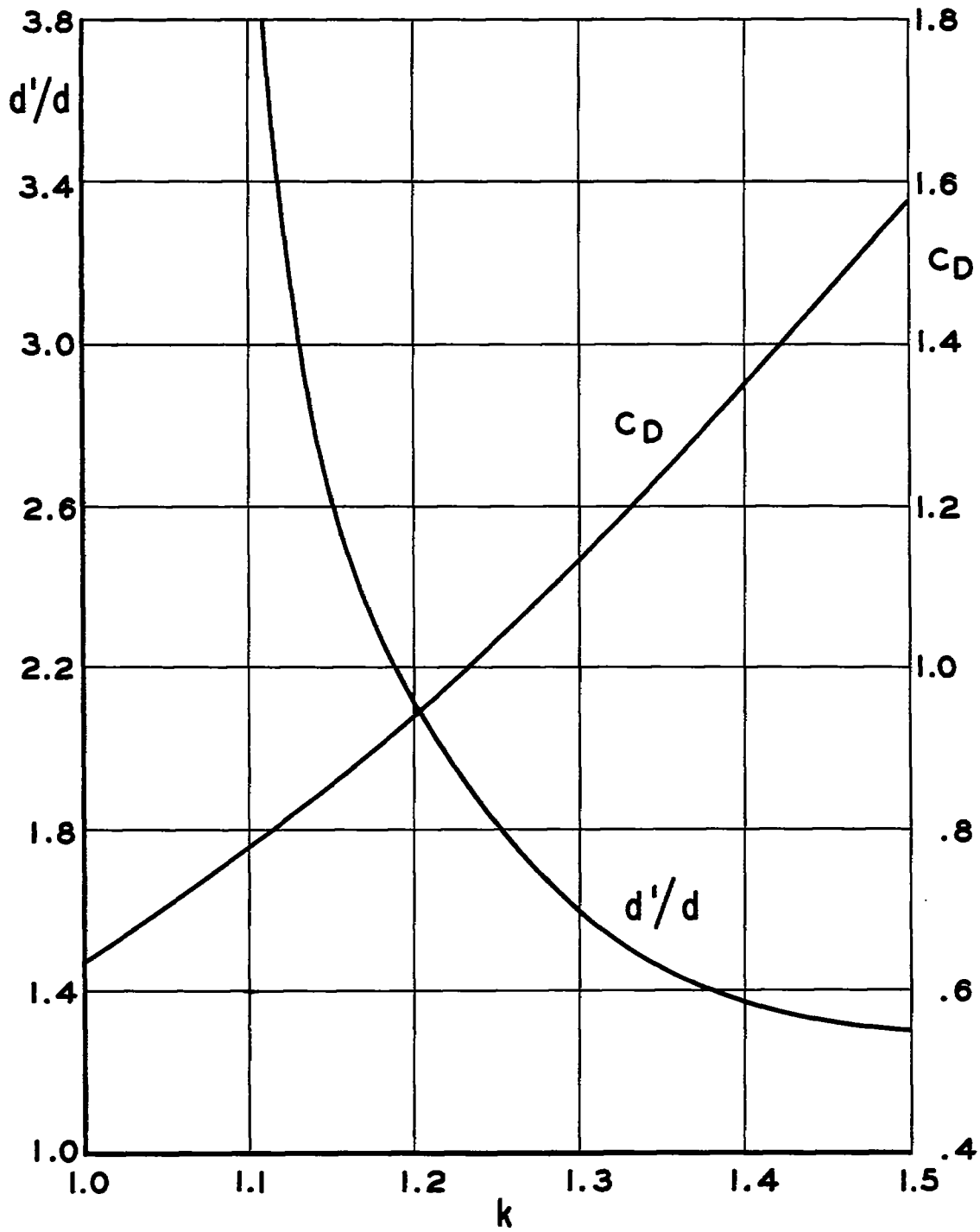

Figure 4.- 90° wedge.

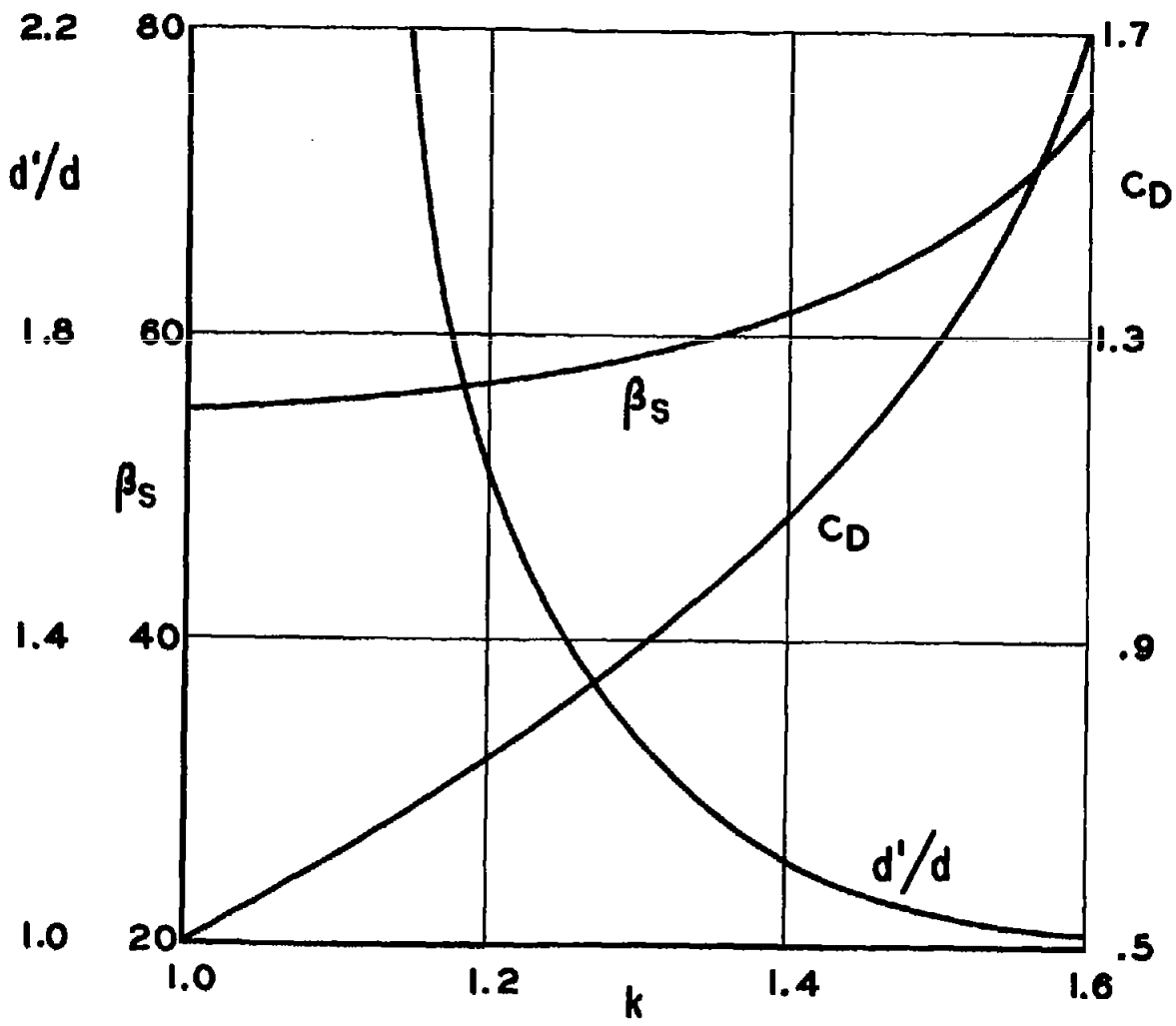

Figure 5.- Circular cylinder.

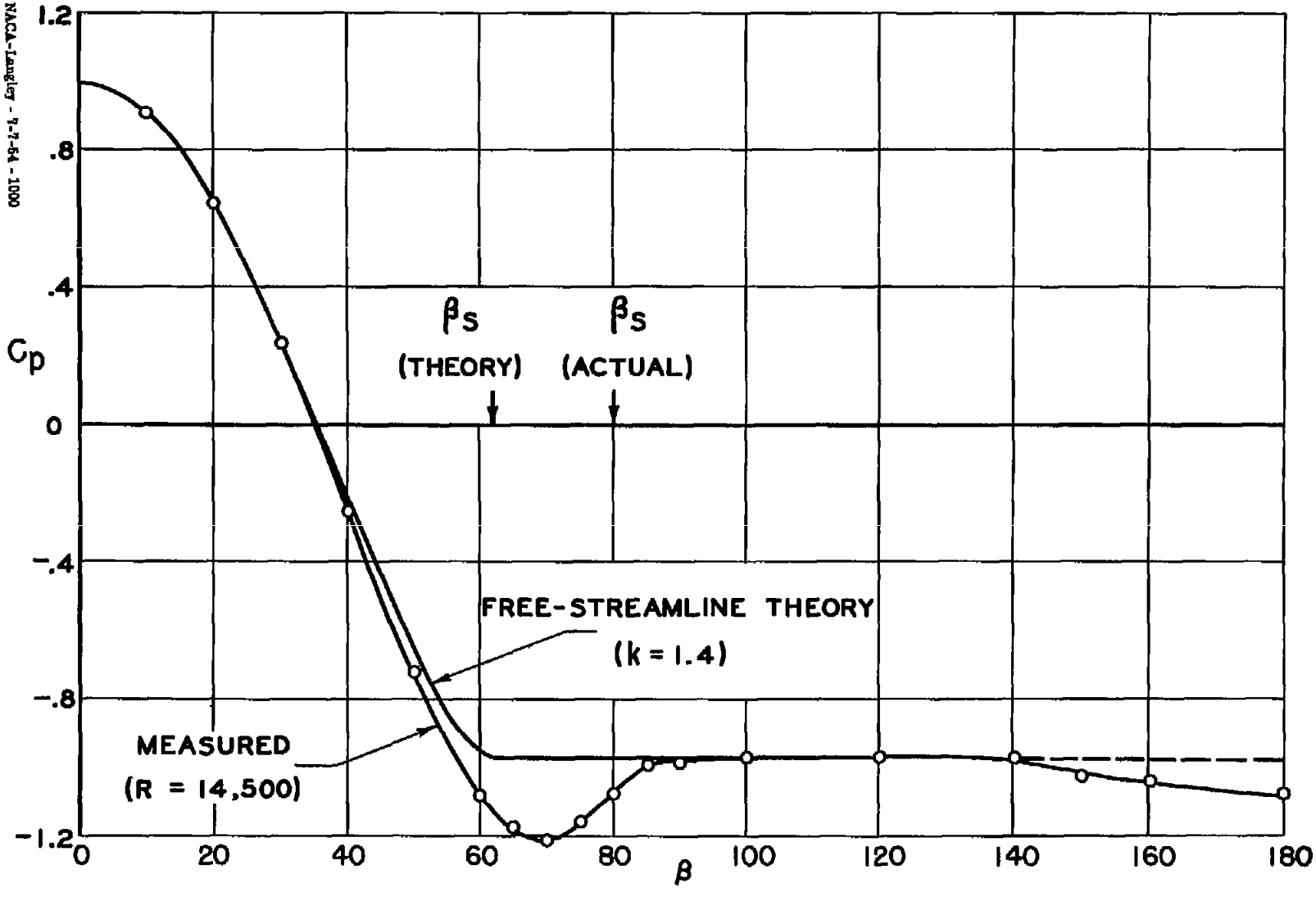

Figure 6.- Pressure distribution on circular cylinder.